Biophysical Chemistry 189 (2014) 16–24

Contents lists available at ScienceDirect

Biophysical Chemistry

journal homepage: http://www.elsevier.com/locate/biophyschem

Protein stabilization and counteraction of denaturing effect of urea by glycine betaine

Narendra Kumar, Nand Kishore *

Department of Chemistry, Indian Institute of Technology Bombay, Powai, Mumbai 400076, India

HIGHLIGHTS

- MD simulation has been used to study the counteraction of denaturing property of urea by glycine betaine.
- Glycine betaine becomes a stronger protecting osmolyte and urea becomes a weaker denaturing agent.
- Increased hydration and decreased interaction of urea with the peptide lead to its counteraction.

GRAPHICAL ABSTRACT

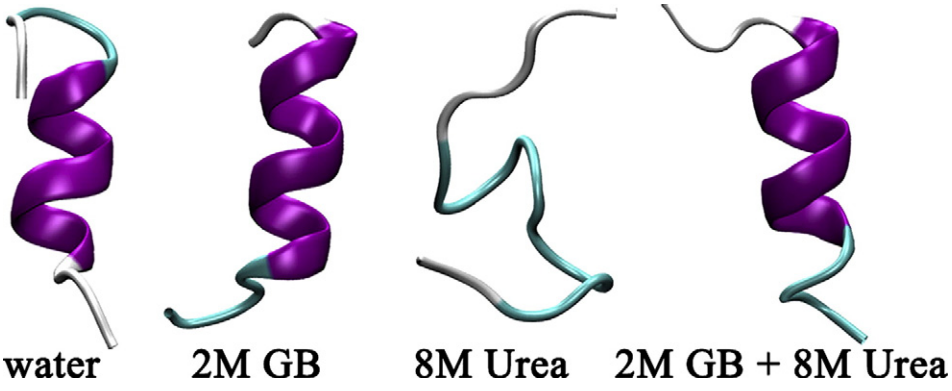

ARTICLE INFO

Article history:
Received 31 January 2014
Received in revised form 7 March 2014
Accepted 10 March 2014
Available online 20 March 2014

Keywords:
S-peptide
Hydrogen bonding
Molecular dynamics simulation
Denaturation
Radial distribution function
Osmolyte

ABSTRACT

The counteraction of the denaturing effect of urea by osmolytes has been one of the most studied problems of osmolyte action. However, the possibility of synergy in osmolyte mixtures has often been neglected. Here, we report synergy in the glycine betaine (GB)–urea mixture by using a model peptide. The results show that in the GB–urea mixture, GB acts as a stronger osmolyte and urea becomes a weaker denaturing agent. This is reflected by an increase in the exclusion of GB from the peptide surface and a decrease in interactions between the peptide and urea. The cause of this synergistic behaviour includes direct interactions between GB and urea through hydrogen bonding, van der Waals interactions between them and strengthening of hydrogen bonding network of water in the GB–urea mixture. The results obtained in this study provide insights into osmolyte induced counteraction of the denaturing effect of urea.

1. Introduction

Severe adverse environmental conditions such as those found in deserts, abyssal water, and icy lands which involve extremely high temperature, high pressure, and high salinity, are far from inhabitable. Nonetheless, nature has bestowed certain mechanisms for the living creatures to survive in such extreme conditions. For example, hyperthermophilic organisms grow optimally above 80 °C, while several barophilic bacteria such as *Psychromonas hadalis* function optimally at a pressure of 500 bar [1–4]. Uncovering the molecular mechanism responsible for this unparalleled adaptability at extreme conditions is of prime importance especially on medicinal and agricultural grounds [4–7]. Small organic molecules such as glycine betaine (GB), called as osmolytes, are known to accumulate with these extremophiles which are a major factor for maintaining their stability and functionality [8,

* Corresponding author.
E-mail address: nandk@chem.iitb.ac.in (N. Kishore).

http://dx.doi.org/10.1016/j.bpc.2014.03.001
0301-4622/

9]. One of the most studied effects of these osmolytes is protection of the native state of proteins from denaturation caused by chemical agents such as urea along with the mechanism of the counteraction of the denaturing effect of urea by osmolytes [9–14]. However, what has often been neglected is "synergy" which can be one of the most important factor in counteracting these extreme conditions. Venkatesu et al. [14] observed that 1 M GB increases the thermal stability of α-chymotrypsin by 6 °C. On the other hand, 1 M urea lowers its thermal stability by 6 °C. However, they further observed that the mixture of 1 M GB and 1 M urea also increases its stability by 6 °C, thus clearly suggesting that GB acts as stronger osmolyte and the denaturation ability of urea reduces in the mixture. This behaviour is an indication of synergy. A similar behaviour was also observed with sarcosine and urea where the authors used the phase diagram method to demonstrate synergy [15]. In a recent study, by using densimetric and activity coefficient data, Rosgen et al. [16] explained the synergy in trimethylamine N-oxide (TMAO)–urea mixtures. They suggested that solvation of TMAO by urea and its strong hydrogen bonding with TMAO–oxygen were the prevalent reasons for synergy. In this study, we account for synergy explicitly by taking a model peptide in the GB–urea mixture and discuss the possible reasons for this synergistic behaviour. The results have implications in designing new synthetic osmolytes which may find uses in the field of medicine, biotechnology, and agriculture [4–7]. To the best of our knowledge, this is the first study providing the molecular explanation for the experimental observations on mixed systems explicitly by studying the possible intermolecular interactions of urea and GB with the peptide. The results are expected to strengthen fundamental research in understanding the behaviour of the mixtures of denaturing agents and osmolytes.

2. Methods

2.1. Simulation system

Molecular dynamics (MD) simulations of an α-helical analogue of the Ribonuclease A S-peptide, Ala–Glu–Thr–Ala–Ala–Ala–Lys–Phe–Leu–Arg–Glu–His–Met–Asp–Ser [17], (Fig. 3) were performed in different solvent systems (Table 1). Our results show agreement with the experimental observations that at 278 K the α-helix of the S-peptide remains stable in aqueous solution [17]. We chose this peptide as it unfolded in the presence of denaturant urea within the range of simulation time, and its smaller size facilitated an in-depth analysis of trajectories. The initial coordinates of the S-peptide were extracted from the first 15 residues of Ribonuclease S (PDB ID: 2RNS) [18]. By 1 Lys/Ala, 9 Glu/Leu, and 1 1Gln/Glu mutations, the final S-peptide was obtained [17,19]. In all the simulations, the OPLS-AA force field was used. The charge parameters of GB were taken from the literature [20]. In all the simulations the simple point charge extended (SPC/E) model [21] was used for water and the Duffy et al. model [22,23] was used for urea following other studies [13,24–26].

Table 1
Details of the simulated systems. M, V, and N indicate molarity, volume, and number of molecules, respectively. Naming of the systems is based on the type of molecules and their concentration present in the system. For example the PU2GB system contains the S-peptide (P), 8 M urea (U) and 2 M glycine betaine (2 GB).

System	$N_{S\text{-}peptide}$	N_{GB}	N_U	N_W	V(nm^3)	M_{GB}(M)	M_U(M)	Time (ns)[a]
P	1			5751	172.6			100(2)
P1GB	1	125		6177	205.1	1.0		100(2)
P2GB	1	261		5836	216.7	2.0		100(2)
PU	1		819	3746	169.1		8.0	100(2)
PU1GB	1	125	1000	3871	206.0	1.0	8.0	100(2)
PU2GB	1	255	990	3005	200.7	2.1	8.2	100(2)

[a] The number of simulations of each system is given in parentheses.

2.2. Simulation details

The GROMACS 4.5.4 molecular dynamics simulation package [27–29] was used to carry out the simulations. An isothermal–isobaric ensemble (NPT) at T = 278 K and P = 1 bar was employed in all the simulations. We used T = 278 K as at this temperature, the S-peptide analogue is known to be in the native form in aqueous solution [17]. The minimum image convention and the periodic boundary conditions were applied in all directions to reduce edge effects. The leap-frog algorithm with a time step of 2 fs was used to integrate the equations of motion. The Berendsen barostat [30] and the v-rescale thermostat [31] were used to control the pressure and temperature with relaxation times of 1 ps and 0.1 ps, respectively. Coordinates were saved in every 4 ps time interval. For each system, a 100 ns trajectory was generated resulting in 25,000 conformations. The simulations were repeated twice for each system with different initial conditions. The LINCS algorithm [32] was used to constrain all the covalent bonds. A cut-off distance of 1.2 nm was employed for non-bonded and for short-range columbic interactions. The Particle Mesh Ewald (PME) method [33] was used to estimate long range electrostatic interactions. Long range dispersion corrections were applied for both energy and pressure.

2.3. Preparation of initial configuration

Multiple steps were applied to prepare the initial configuration and to equilibrate the systems before the production runs. First, a cubic box of water was created by using the genbox utility of GROMACS [28] and, then 1 M GB, 2 M GB, 8 M urea, 1 M GB + 8 M urea, and 2 M GB + 8 M urea aqueous systems were created by randomly placing required numbers of urea and GB molecules, and removing the vicinal water to get the required concentrations of GB and urea. These systems were the steepest-descent energy minimized for 10,000 steps and then equilibrated for 10 ns each in NPT ensembles at T = 278 K and P = 1 bar. The S-peptide was the steepest-descent energy minimized for 5000 steps in vacuo and then it was placed in the centre of the box of the above generated systems containing water, GB + water, and GB + urea + water. Two different sets of final inputs for the production runs were created by variations in the further steepest-descent energy minimization and position-restrained MD simulation steps. For example, the first set of the final input was created by energy minimization of 10,000 steps of the whole system, and then further 20 ps of position-restrained MD where position restraints were applied on the S-peptide only. In the second set of the final input, energy minimization was done for 5000 steps and then 40 ps of position restrained MD was performed. These inputs were used for the production runs.

2.4. Preferential interaction coefficient

The preferential interaction coefficient (Γ_{XP}) provides a measure of the excess number of cosolute molecules present in the vicinity of a protein with respect to water. The positive value of Γ_{XP} indicates the preferential interaction and its negative value indicates the preferential exclusion of cosolute from a protein surface. The Γ_{XP} value of a cosolute is related to Gibbs free energy of transfer of a protein from aqueous solution to cosolute environment [34]. The value of Γ_{XP} can be calculated by using the following equation [24,34–36]:

$$\Gamma_{XP} = \left\langle n_X^{I} - n_W^{I}\left(\frac{n_X^{II}}{n_W^{II}}\right)\right\rangle. \quad (1)$$

Here, n_X and n_W are the number of a particular cosolute and water molecules, respectively. I and II represent regions in the vicinity of a protein and bulk, respectively. The cut-off distance of 0.45 nm was used following RDFs between different atoms of the S-peptide and cosolute atoms [4].

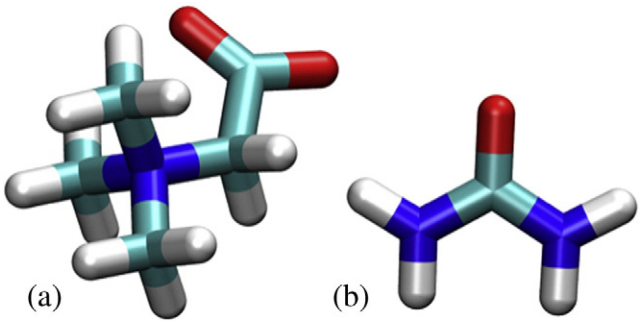

Fig. 1. Molecular structure of (a) glycine betaine, and (b) urea. Red, blue, cyan and grey colours indicate oxygen, carbon, nitrogen, and hydrogen atoms, respectively.

3. Results and discussion

3.1. Structure of S-peptide in different systems

Details of the simulated systems are provided in Table 1. To understand whether GB (Fig. 1) can offset the denaturing effect of urea, the C_α-root mean square deviation (RMSD) of the S-peptide was plotted as a function of time for all the simulated systems (Fig. 2). We found that the S-peptide remained significantly stable in the aqueous (P), 1 M GB (P1GB), 2 M GB (P2GB), 1 M GB + 8 M urea (PU1GB), and 2 M GB + 8 M urea (PU2GB) systems. However, in the presence of 8 M urea (system PU), the RMSD increased by 200% with respect to its aqueous counterpart after 45 ns of the simulation indicating unfolding (denaturation) of the peptide. The presence of 1 M or 2 M GB in 8 M urea solution was able to restore the native form of the peptide. In other words, these mixtures were capable to counteract the denaturing effect of urea. In Fig. 3, conformations of the S-peptide are shown for all the systems after 100 ns of the simulation along with its initial structure. Here, the S-peptide conformations for all the systems are significantly similar to their initial conformations except for the PU1GB system where the peptide conformation is partially denatured, and for the PU system where the conformation turns into "turn". This confirms that 1 M GB was able to partially counteract, and 2 M GB was able to fully counteract the denaturing effect of urea.

To examine the conformational stability of the S-peptide in different solvent environments, the secondary structure was calculated for all the systems shown in Fig. 4 by using the DSSP programme [37]. The secondary structure remained almost the same for the P, P1GB, P2GB, and PU2GB systems. However, for the PU1GB system, the α-helix of the peptide was partially lost and for the system PU, at 45 ns, there was a sharp transition which indicated complete loss of α-helix and the S-peptide turned into "turn" and "coil" secondary structure. Here, the presence of 2 M GB in 8 M urea solution (PU2GB) was fully able to offset the denaturing effect of urea. These results are in agreement with experimental findings where GB was able to counteract the denaturing effect of urea for different proteins [9,10,14,38].

In the rest of the sections, the analysis of the trajectories was restricted to folded state of the S-peptide as the accessibility of the S-peptide for cosolvents changes from folded to unfolded (denatured) state. This was done by analysing the trajectories from 1 ns to 40 ns for the system PU as in this range the S-peptide remains in fully folded state. In the system PU1GB, the S-peptide remains in partially folded state, therefore, this system has not been used for comparison of the properties. For the rest of the systems, the S-peptide remains in fully folded state, therefore, a whole range of the simulation time was taken for the analysis of the properties.

3.2. Synergistic effects of GB-urea mixture

3.2.1. Preferential exclusion of GB and preferential interaction of urea

The values of preferential interaction coefficient (Γ_{XP}) of GB and urea for the S-peptide were calculated to understand the preferential interaction and exclusion of the cosolute molecules with the S-peptide. The values of Γ_{XP} for GB are negative and positive for urea in all the studied systems (Table 2) which indicate that GB is preferentially excluded from the S-peptide surface and urea preferentially interact with the S-peptide. This is in agreement with the literature that the protecting osmolyte such as GB is excluded from protein surface and denaturing agent such as urea preferentially interacts with proteins [11,12,39,40]. Here, we see that the presence of urea increases the exclusion of GB from the S-peptide surface which is clear from the decrease in the Γ_{XP} value of GB (Table 2). For example the Γ_{XP} value of GB in the system P2GB is −0.63 which decreases to the value of −2.89 in the presence of urea (system PU2GB). Similarly, in the presence of GB, the Γ_{XP} value of urea decreases. For example, for the PU system, the value of Γ_{XP} for urea is 14.69 which is decreased to the value of 3.20 in the presence of GB (system PU2GB). These findings suggest that urea increases the exclusion of GB, therefore, strengthens its ability as a protecting osmolyte and the presence of GB decreases the interaction of urea with the S-peptide, therefore, weakens its denaturing property. In other words, GB becomes a stronger protecting osmolyte and urea becomes a weaker denaturing agent indicating synergy in the GB–urea mixture. Similar trends are observed for the Γ_{XP} value for the S-peptide backbone (Table 2). The presence of GB molecules decreases the number of urea molecules in a shell of 0.45 nm from the S-peptide surface and vice-versa (Table 2) which again supports synergy in the GB–urea mixture.

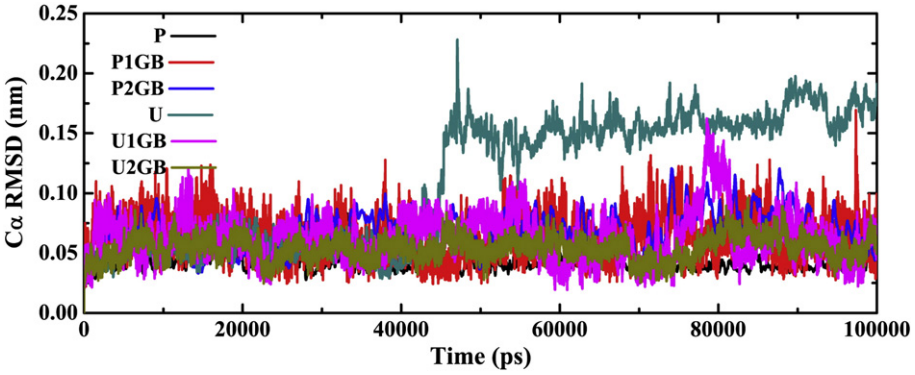

Fig. 2. Root mean square deviation (RMSD) of α-carbon of S-peptide helix (from residue 4–11). An increase in the α-RMSD for the 8 M urea solution (PU) of about 200% is observed after 45 ns of simulation which indicates unfolding of the S-peptide.

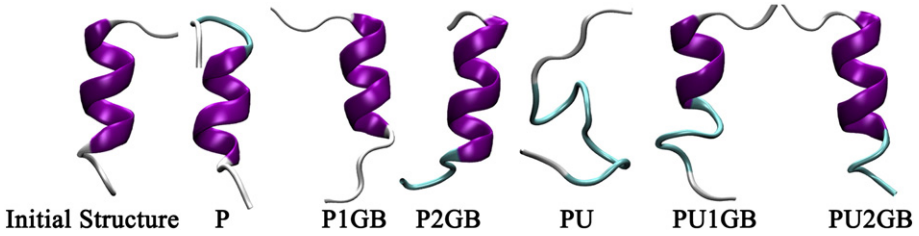

Fig. 3. Conformation of S-peptide after 100 ns of simulation along with initial structure. The S-peptide structure is similar to the initial structure for the systems except in the 8 M urea solution where the α-helix is completely lost.

The Γ_{XP} value of denatured state of the S-peptide was found to be 7.81. To compare our result from the literature, Gibbs free energy of transfer per peptide bond of the backbone from water to 1 M urea or 1 M GB solution was calculated using the following equation [34,41]:

$$\Delta\mu^{tr} = -RT\frac{\Gamma_{XP}}{14c} \quad (2)$$

where $\Delta\mu^{tr}$ is the Gibbs free energy of transfer from water to 1 M urea or GB solution with 14 peptide bonds present in the S-peptide. Here c represents the molar concentration of GB or urea present in the system. From the above equation, the value of $\Delta\mu^{tr}$ for urea was calculated to be −38.5 cal mol^{-1} which matches with the experimental value of −39 cal mol^{-1} [42]. The Γ_{XP} value of GB for the P2GB system is −1.96 (Table 2) which corresponds to 38.7 cal mol^{-1} which is less than the experimental value of 67 cal mol^{-1}. This difference is expected as in the P2GB system, we are dealing with the folded state of the S-peptide, therefore, it will be partially inaccessible to the solvent molecules.

The negative value of Γ_{XP} of GB for most of the residues of the S-peptide for the system P2GB and similarly, the positive value of Γ_{XP} of urea for the system PU are in accordance with literature [4] (Fig. 5).

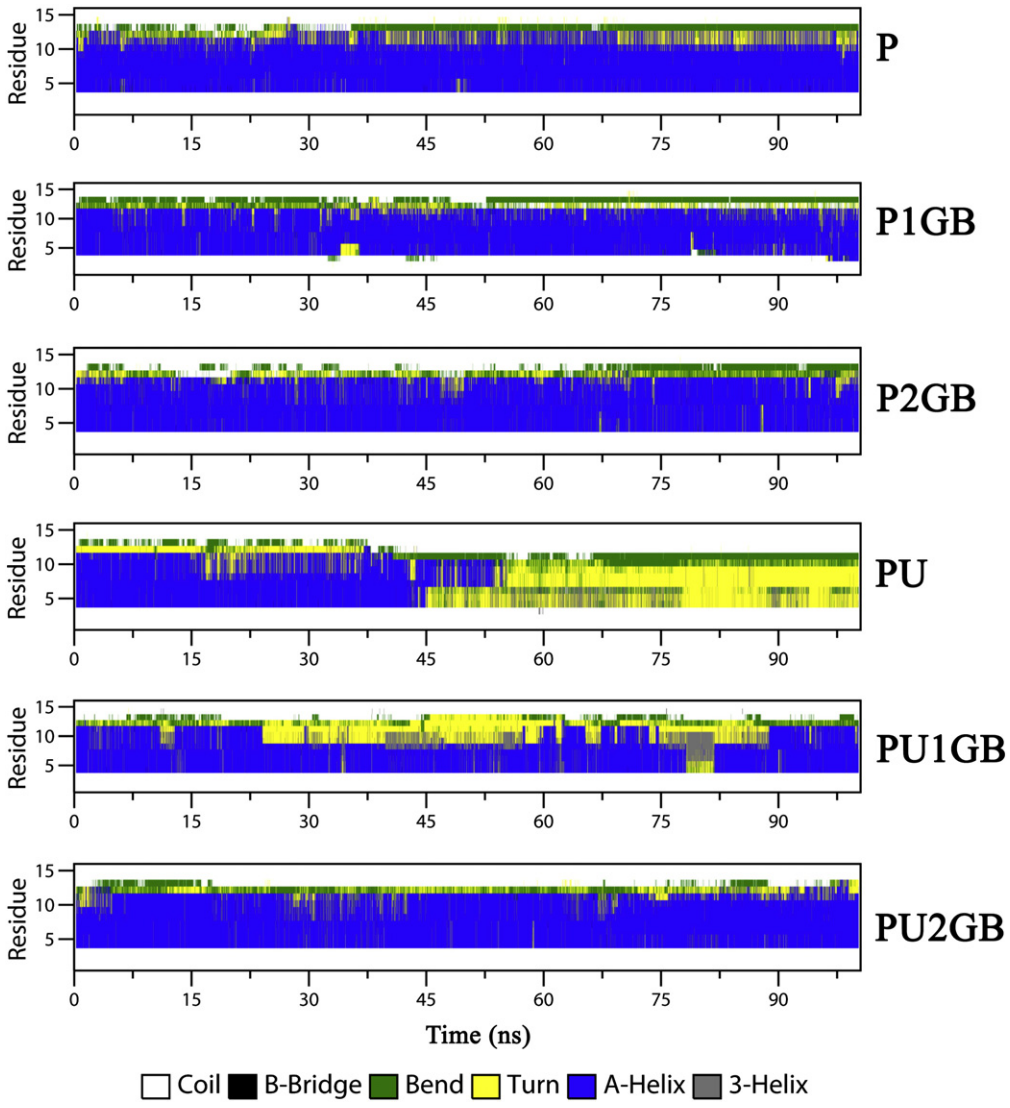

Fig. 4. Secondary structure of the S-peptide in different systems. The secondary structure remains similar for all the systems except for 8 M urea solution (PU), where α-helix is lost completely after 45 ns of the simulation.

Table 2
Preferential interaction coefficient[b] (Γ_{XP}) of GB and urea for the S-peptide and its backbone along with the number of urea (N_{urea}) and GB (N_{GB}) molecules present in a shell of radius 0.45 nm from the S-peptide surface.

System	S-peptide				S-peptide backbone			
	Γ(GB)	Γ(Urea)	N_{urea}	N_{GB}	Γ(GB)	Γ(Urea)	N_{urea}	N_{GB}
P2GB	−0.63			6.21	−1.96			0.15
PU		14.69	36.87			5.70	12.90	
PU2GB	−2.89	3.20	32.62	4.80	−2.28	2.56	11.54	0.06

[b] Maximum error associated in the calculation of Γ_{XP} was 10%.

Table 3
Number of hydrogen bonds formed between different molecules for all the systems.

System	Peptide–GB	Peptide–urea	GB–urea	Peptide–water
P2GB	4 ± 1			47 ± 2
PU		20 ± 1		32 ± 2
PU2GB	2 ± 1	16 ± 1	424 ± 4	34 ± 2

The decrease in the values of Γ_{XP} of GB for most of the residues of the S-peptide from the system P2GB to PU2GB (Fig. 5) indicates that the presence of urea increases the exclusion of GB from most of the S-peptide residues. The significant positive values of Γ_{XP} of urea for the most of the residues of the S-peptide for the system PU indicate that urea is mostly accumulated at all the S-peptide residues. However, when urea is taken in the presence of GB (system PU2GB), the values of Γ_{XP} of urea for the residues Leu9, Arg10, Met13, Asp14, and Ser15 of the S-peptide become negative indicating exclusion of urea from these residues. This exclusion of urea from these residues might contribute in maintaining the stability of the S-peptide in the presence of urea (Fig. 5). The value of Γ_{XP} of GB and urea for backbone residues of the S-peptide showed the same trends as S-peptide residues (Fig. S1 of Supplementary information).

3.2.2. Hydrogen bonding interactions

Hydrogen bonding interactions play an important role in protein stabilization [12]. According to Jaffrey's classification [43], H bonding interactions are electrostatic in nature. As urea does not have any overall net charge, the electrostatic interactions between urea and S-peptide can be considered as H bonding interactions [44]. The average number of H bonds formed between the S-peptide and urea is provided in Table 3. Here, the H bond length cut-off distance of 0.35 nm and a maximum donor-hydrogen-acceptor angle of 30° were taken to define hydrogen bond following other studies [45,46]. The number of H bonds between the S-peptide and urea decreased in the presence of GB. For example, when moving from the system PU to PU2GB, the S-peptide–urea H bonds decreased from (20 ± 1) to (16 ± 1). However, given the error associated with the calculation of the number of H bonds between GB and the S-peptide, it is difficult to draw any conclusion on the effect of urea in the H bonding interaction of GB and the S-peptide (Table 3). The decrease in the number of H bonds between urea and the S-peptide in the GB–urea mixture leads to an enhanced hydration of the peptide hence increasing its stability. The average number of H bonds between urea and GB per GB molecule was found to be 1.66 for the system PU2GB (Table 3), indicating direct interaction of urea with GB through H bonding interactions between the oxygen atom of GB and hydrogen atom of urea. This accounts for the reduced H bonding interactions between S-peptide and urea. Interaction of urea with GB might also help in keeping GB away from the S-peptide surface. The number of H bonds formed by the S-peptide with GB and urea as a function of time for different systems are plotted in Fig. 6. The number of H bonds between the S-peptide and urea for the system PU and PU2GB clearly indicates that the presence of GB causes a decrease in the H bonding interaction between the S-peptide and urea. From these results, it can be concluded that the H bonding interactions play a major role in the observed synergy in GB–urea mixtures.

3.2.3. Role of direct interactions in synergy

The average S-peptide–GB and S-peptide–urea electrostatic and van der Waals (vdw) interaction energies were calculated to probe the possible role of direct interactions in the synergy of GB–urea mixtures (Table 4). A decrease in the S-peptide–GB and S-peptide–urea electrostatic and vdw interaction energies from the systems P2GB and PU to PU2GB, indicates an increase in exclusion of GB and decrease in the favourable interactions between S-peptide and urea. We see that the vdw interaction energy between S-peptide and GB decreased by 31% from the system P2GB to the system PU2GB in comparison to 13.8% decrease of corresponding electrostatic interaction energy. The S-peptide–urea vdw interaction energy decreased by 20% from system PU to the system PU2GB in comparison to a 24% decrease in the electrostatic interactions. The highest 31% decrease in the S-peptide–GB vdw interactions suggests that urea excludes GB from the S-peptide surface mostly by decreasing the vdw interactions between the S-peptide and GB. The osmolyte GB has a slightly higher impact on the S-peptide–urea electrostatic interaction than the vdw interactions which suggests that GB can directly interact with urea through electrostatic as well as H bonding interactions. A total decrease of 44.8% in the interaction energy between the S-peptide and GB for the 2 M GB system is almost equivalent to the decrease of 44% in the S-peptide and urea interaction energy (Table 4). Thus it will be interesting to know at what composition of cosolutes, the synergy will be at maximum.

3.2.4. Radial distribution functions

The radial distribution function (RDF) is a measure of the density and arrangement of one type of molecule around another molecular species. To show the exclusion of GB and synergy in the GB–urea mixture; peptide–urea, peptide–GB RDFs for the systems PU, P2GB, and PU2GB were plotted in Fig. 7a. Here, from the peptide–GB RDF, we see that for the system PU2GB, GB is excluded more from the S-peptide surface than for the system P2GB. From the peptide–urea RDF, the density of urea around the S-peptide is decreased from the system PU to the

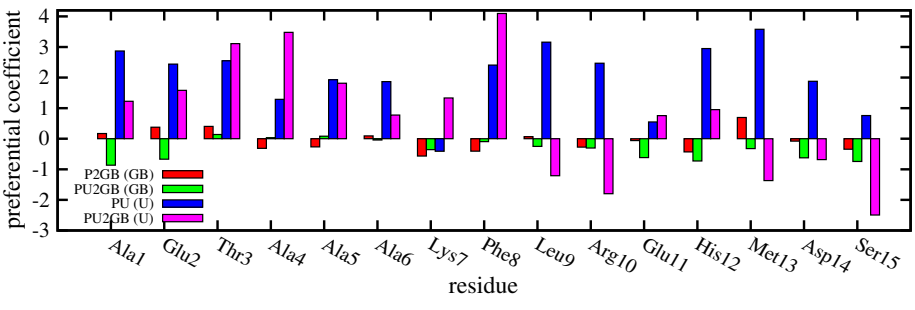

Fig. 5. Preferential interaction coefficient of GB and urea for all the residues of S-peptide in different systems.

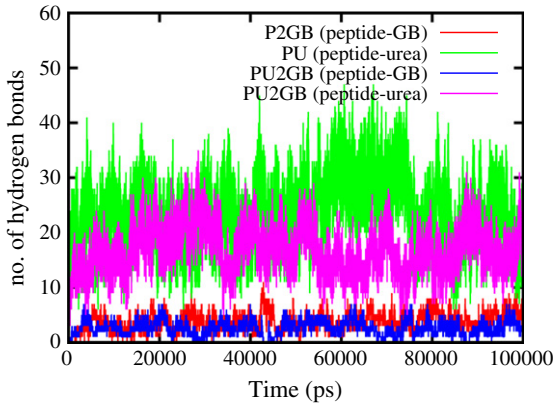

Fig. 6. Number of S-peptide–urea and S-peptide–GB H bonds as a function of time. GB causes a substantial decrease in the H bond interaction between urea and the S-peptide.

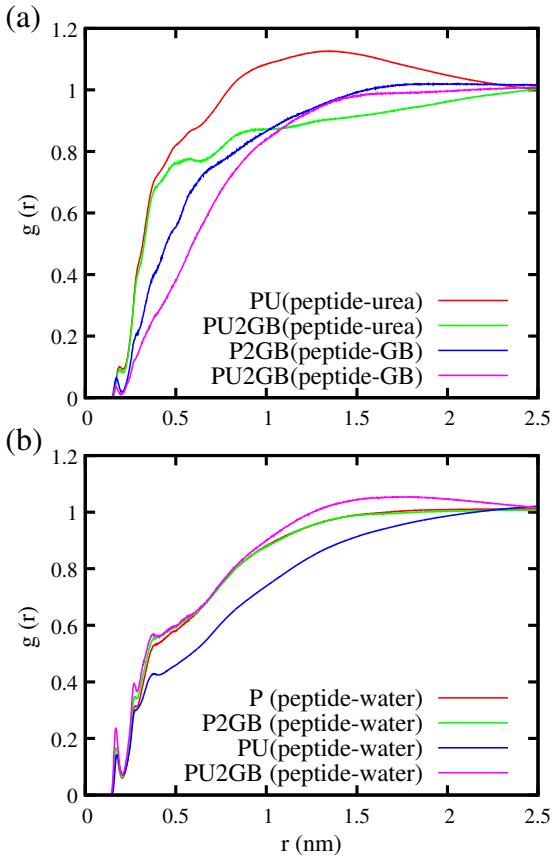

Fig. 7. Radial distribution function between S-peptide and (a) urea and GB, (b) water. For system PU2GB, the exclusion of GB from the S-peptide is increased compared to the P2GB system and there is decrease in the urea density above 0.4 nm in comparison to the PU system which shows synergy in the GB–urea system.

system PU2GB after 0.4 nm of the distance from the S-peptide. This decrease in the density of urea and increase in the exclusion of GB indicate synergy. The peptide–water RDFs are shown in Fig. 7b for different systems. It is interesting to note that among all the systems the water density is the highest for the system PU2GB and minimum for the system PU, which indicates that the hydration of the S-peptide is decreased in the presence of urea. However, it is at maximum in the GB–urea mixtures. It is established that, preferential hydration of the protein, is a the major factor leading to stabilization of proteins [12,47]. These findings are in agreement with the observations based on Γ_{XP} values.

To understand different types of interactions between the S-peptide and urea, the RDFs between relevant atoms of the S-peptide and urea are plotted in Fig. 8. The RDF between backbone carbonyl group oxygen (OB) and urea nitrogen (NU) is decreased in the presence of GB (Fig. 8a). The first peak of this RDF corresponds to hydrogen bonding interactions between OB and hydrogen atoms of urea molecule. This decrease is due to direct interactions between urea and GB as clear from the GB oxygen–urea nitrogen (OG–NU) RDF (Fig. 9) which is in agreement with experimental findings on GB and urea [48]. The first peak of this OG–NU RDF for the system PU2GB corresponds to hydrogen bonding between GB and urea, and a significant second peak of the GB methyl carbon–urea carbon (CG–CU) RDF is an indication of strong vdw interactions between GB and urea. This is supported by highly negative values of electrostatic and vdw interaction energies between them (Table 4).

When moving from the PU to the PU2GB system, we see only a slight change in the first peak of the backbone nitrogen and urea oxygen (NB–OU) RDF (Fig. 8b) as GB is unable to make any H bonds with oxygen atoms of urea molecules. However, we do see an overall substantial decrease in the NB–OU RDF which can be due to strong vdw interactions between GB and urea. As these interactions would lead to decrease in the density of urea around the S-peptide. In Fig. 8c, when moving from PU to PU2GB, a small decrease in the first peak of RDF between negatively charged side chain oxygen atoms (ON) and urea nitrogen atoms (NU), indicates loss in H bonding between ON and NU.

Again we see a substantial decrease in the RDF between positively charged nitrogen atoms of the side chains (NP) and urea oxygens (OU) in the presence of GB. This decrease can be attributed to competition between hydrogen bonding of NP with OU and OG (GB oxygen) (Fig. 8d) as the side chain nitrogen atoms of Lys7, Arg10, and His12 of the S-peptide are far from the backbone, that can be easily accessed by GB (Fig. 10) providing strong competition to urea.

To examine the S-peptide and GB interactions, the relevant RDFs for the systems P2GB and PU2GB are shown in Fig. 11. In Fig. 11a, a sharp first peak in the P2GB system indicates that GB interacts with the backbone nitrogen (NB) through hydrogen bonding. However, in the presence of urea (PU2GB), this H bond interaction is immensely decreased. This decrease can be explained as GB and urea strongly interact with each other (Table 4), therefore, the availability of GB around the S-peptide decreases, thus decreasing the first peak of NB–OG RDF which results in the exclusion of GB from the surface of the S-peptide in the presence of urea (system PU2GB). In the positively charged side chain nitrogen atoms of the S-peptide and GB oxygen (NP–OG) RDF (Fig. 11b), a very significant sharp first peak is observed pointing out strong hydrogen bonding interactions between the hydrogen atom of the NP and OG. The first peak of the NP–OG RDF increases in the

Table 4
Electrostatic (E_E) and van der Waals (E_{vdw}) interaction energies between different molecules in kJ mol^{-1}.

System	Peptide–GB		Peptide–urea		GB–urea	
	E_E	E_{vdw}	E_E	E_{vdw}	E_E	E_{vdw}
P2GB	−174 ± 7	−82 ± 3				
PU			−853 ± 39	−475 ± 15		
PU2GB	−150 ± 7	−57 ± 4	−649 ± 16	−367 ± 8	−10,589 ± 65	−5573 ± 8

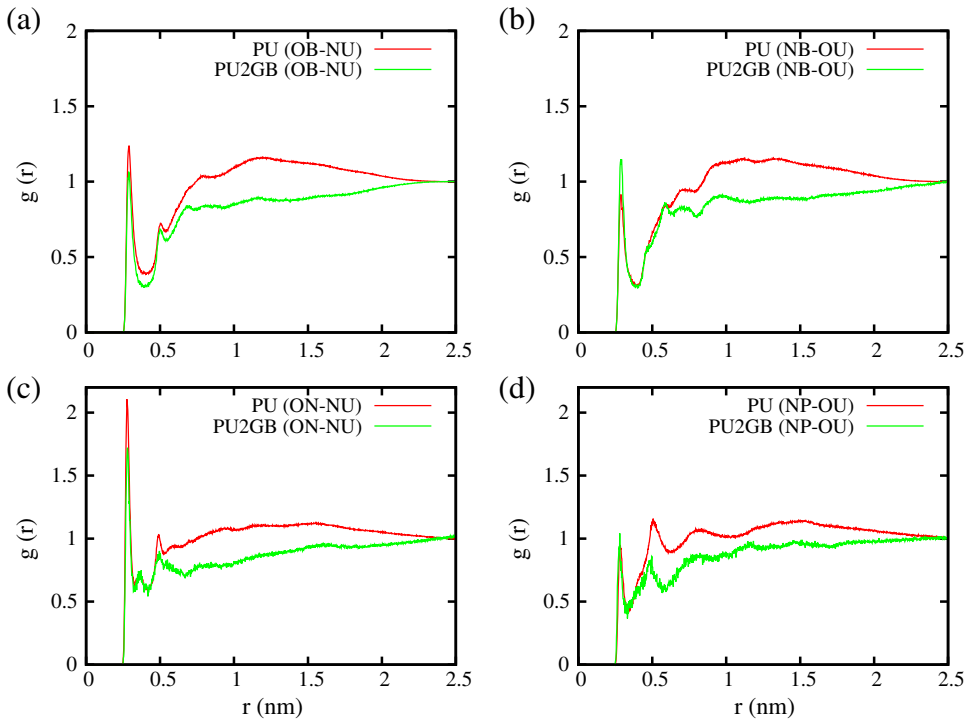

Fig. 8. S-peptide–urea radial distribution functions. Here OB and NB represent backbone oxygen and nitrogen atoms of the S-peptide, respectively. Similarly, ON and NP denote negatively charged side chain oxygen and positively charged nitrogen atoms of the S-peptide. NU and OU represent nitrogen and oxygen atoms of urea, respectively.

presence of urea (PU2GB system) which means that the presence of urea increases the S-peptide and GB interaction. This increase can be explained as the presence of urea excludes GB from the backbone of the S-peptide and the nitrogen containing amino acid residues Lys7, Arg10, and His12 of the S-peptide are exposed to the solvent medium (Fig. 10). Therefore, it is more probable that GB will interact more with positively charged side nitrogen atoms (NP) in the system PU2GB than the system P2GB.

The vdw interaction energy plays an important role in protein stabilization [11]. To understand the effect of GB on the S-peptide–urea vdw interaction energy, the RDF between Cβ atoms of amino acid residues and the carbon atom of urea (Cβ–CU) is plotted in Fig. 11c. We see that the addition of GB decreases the Cβ–CU RDF and hence the vdw interaction energy between the S-peptide and urea. In Fig. 11d, the RDF between Cβ of the S-peptide and GB methyl carbon (Cβ–CG) is plotted. Here, we observe that addition of urea results in collapse of the second peak of the RDF which means a decrease in the vdw interaction energy, or in other words more exclusion of GB from the S-peptide surface.

Increase in water structure and its H bonding network are associated with an increase in protein stabilization [26,47]. To show the combined effect of GB–urea mixtures on water structure, the RDFs between water oxygen atoms (OW–OW) for different systems are depicted in Fig. 12. We found that GB, urea, and the GB–urea mixture increased the first peak of the OW–OW RDF indicating an increase in water structure and H bonding interactions between water molecules. However, the increase in water structure in the GB–urea mixture was higher than the combined increase for GB and urea separately which indicates increased S-peptide stabilization, hence, occurrence of synergy in the GB–urea mixture.

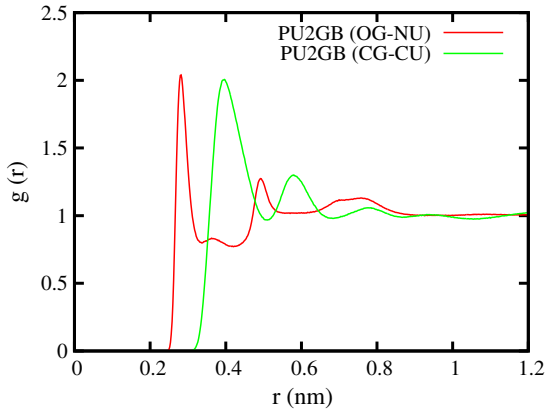

Fig. 9. Radial distribution function between GB and urea. OG and CG represent oxygen and methyl carbon atoms of GB, respectively. Similarly, CU and NU represent carbon and nitrogen atoms of urea molecules. Strong peaks for both the RDFs indicate a strong direct interaction between GB and urea through H bonding and vdw interactions.

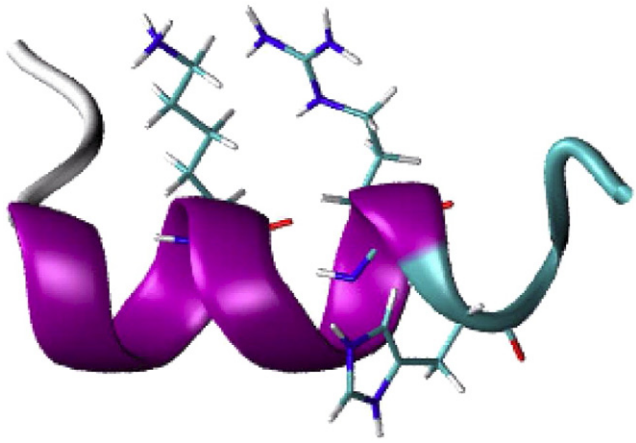

Fig. 10. S-peptide and with Lys7, Arg10, and His12 residues.

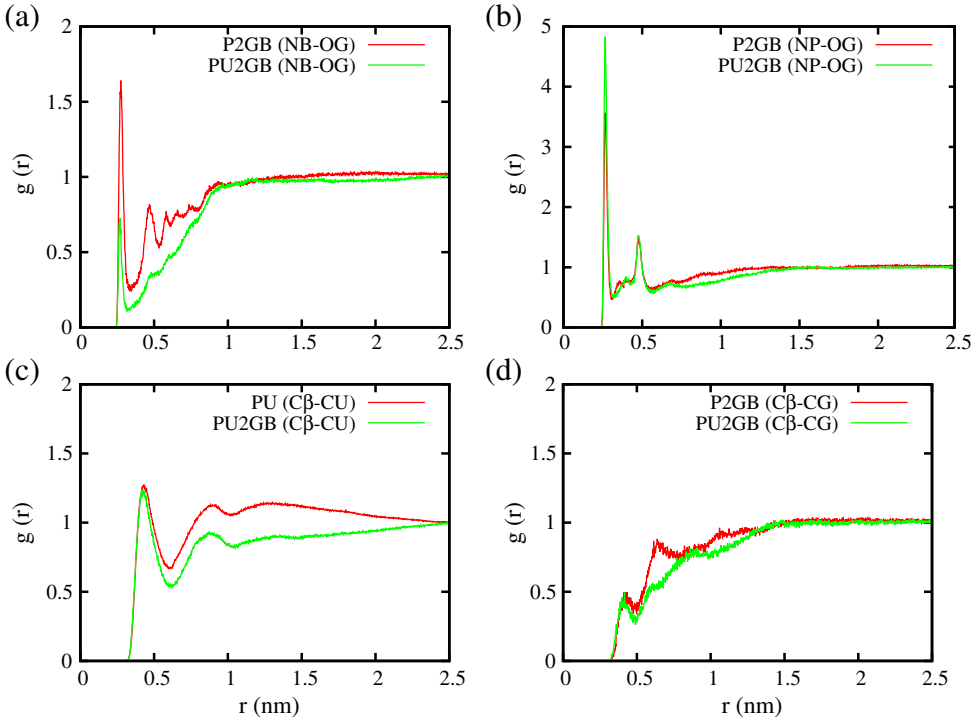

Fig. 11. S-peptide–GB and S-peptide–urea radial distribution functions. NB, NP, and Cβ represent backbone nitrogen, positively charged side chain nitrogen and β carbon atoms of the S-peptide, respectively. OG and CG represent oxygen and methyl group carbon atoms of glycine betaine, respectively, whereas CU represents the carbon atom of urea molecules. The results show that urea increases the exclusion of GB by substantially decreasing the H bonding and vdw interactions between S-peptide and urea.

4. Conclusions

In this study, we have used molecular dynamics simulations to account for the synergy in GB–urea mixtures in terms of counteraction of the denaturing effect of urea by using a model S-peptide. A molecular explanation for the experimental observations on the mixed systems has been provided. Our results support both a direct [49–52] and an indirect mechanism [12,26,47,53,54] of protein stabilization by osmolytes. We find that in the GB–urea mixtures, the exclusion of GB from the S-peptide surface is substantially increased and interaction of urea with the S-peptide backbone, which is considered as the main cause of protein denaturation [49,51], is enormously decreased. This synergistic behaviour is due to an increased hydration of the S-peptide, a decreased interaction of GB and urea with the S-peptide, and direct interactions between GB and urea through H bonding and vdw interactions in the GB–urea mixture. Finally, the results obtained in this study provide insights into osmolyte induced counteraction of the denaturing effect of urea.

It will be interesting to extend the work with different osmolytes to understand their combined effects to protect the native states of proteins. Similarly a mixture of denaturing agents might prove to be more effective in killing parasites, thus improving agricultural production [4–6].

Supplementary data to this article can be found online at http://dx.doi.org/10.1016/j.bpc.2014.03.001.

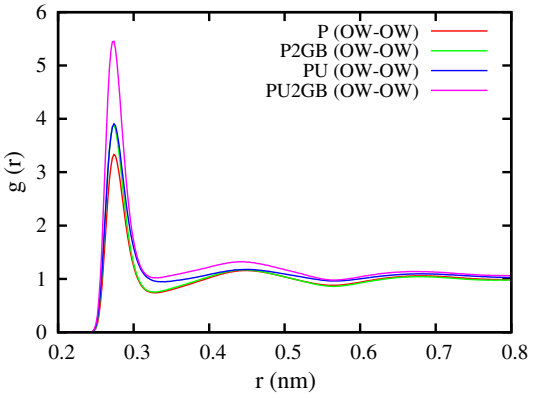

Fig. 12. Water oxygen–oxygen (OW–OW) radial distribution function for different systems. H bonding network of water is strengthened more than for urea and GB solution separately.

Acknowledgments

Computing time from IIT Bombay computer centre is gratefully acknowledged. N. Kumar acknowledges CSIR, New Delhi for a Senior Research Fellowship.

References

[1] A.A. Yayanos, A.S. Dietz, R.V. Boxtel, Isolation of a deep-sea barophilic bacterium and some of its growth characteristics, Science 205 (1979) 808–810.
[2] C. Vieille, G.J. Zeikus, Hyperthermophilic enzymes: sources, uses, and molecular mechanisms for thermostability, Microbiol. Mol. Biol. Rev. 65 (2001) 1–43.
[3] E.F.F. Delong, D.G.G. Franks, A.A.A. Yayanos, Evolutionary relationships of cultivated psychrophilic and barophilic deep-sea bacteria, Appl. Environ. Microbiol. 63 (1997) 2105–2108.
[4] G. Saladino, S. Pieraccini, S. Rendine, T. Recca, P. Francescato, G. Speranza, M. Sironi, Metadynamics study of a β-hairpin stability in mixed solvents, J. Am. Chem. Soc. 133 (2011) 2897–2903.
[5] A. Furini, C. Koncz, F. Salamini, D. Bartels, High level transcription of a member of a repeated gene family confers dehydration tolerance to callus tissue of *Craterostigma plantagineum*, EMBO J. 16 (1997) 3599–3608.
[6] X. Deng, J. Phillips, A.H. Meijer, F. Salamini, D. Bartels, Characterization of five novel dehydration-responsive homeodomain leucine zipper genes from the resurrection plant *Craterostigma plantagineum*, Plant Mol. Biol. 49 (2002) 601–610.
[7] P.H. Yancey, Organic osmolytes as compatible, metabolic and counteracting cytoprotectants in high osmolarity and other stresses, J. Exp. Biol. 208 (2005) 2819–2830.
[8] P.H. Yancey, M.E. Clark, S.C. Hand, R.D. Bowlus, G.N. Somero, Living with water stress: evolution of osmolyte systems, Science 217 (1982) 1214–1222.

[9] P.H. Yancey, G.N. Somerot, Counteraction of urea destabilization of protein structure by methylamine osmoregulatory compounds of elasmobranch fishes, Biochem. J. 183 (1979) 317–323.
[10] M.B. Burg, E.M. Peters, K.M. Bohren, K.H. Gabbay, Factors affecting counteraction by methylamines of urea effects on aldose reductase, Proc. Natl. Acad. Sci. 96 (1999) 6517–6522.
[11] N. Zhang, F.-F. Liu, X.-Y. Dong, Y. Sun, Molecular insight into the counteraction of trehalose on urea-induced protein denaturation using molecular dynamics simulation, J. Phys. Chem. B 116 (2012) 7040–7047.
[12] B.J. Bennion, V. Daggett, Counteraction of urea-induced protein denaturation by trimethylamine N-oxide: a chemical chaperone at atomic resolution, Proc. Natl. Acad. Sci. 101 (2004) 6433–6438.
[13] F. Meersman, D. Bowron, A.K. Soper, M.H.J. Koch, Counteraction of urea by trimethylamine N-oxide is due to direct interaction, Biophys. J. 97 (2009) 2559–2566.
[14] P. Venkatesu, M.-J. Lee, H.-m. Lin, Osmolyte counteracts urea-induced denaturation of r-chymotrypsin, J. Phys. Chem. B 113 (2009) 5327–5338.
[15] L.M.F. Holthauzen, M. Auton, M. Sinev, J. Rösgen, Protein stability in the presence of cosolutes, Methods Enzymol. 492 (2011) 61–125.
[16] J. Rösgen, R. Jackson-Atogi, Volume exclusion and H-bonding dominate the thermodynamics and solvation of trimethylamine-N-oxide in aqueous urea, J. Am. Chem. Soc. 134 (2012) 3590–3597.
[17] J. Tirado-rives, W.L. Jorgensen, Molecular dynamics simulations of the unfolding of an a-helical analogue of ribonuclease A S-peptide in water, Biochemistry 30 (1991) 3864–3871.
[18] E.E. Kim, R. Varadarajan, H.W. Wyckoff, F.M. Richards, Refinement of the crystal structure of ribonuclease S. Comparison with and between the various ribonuclease A structures, Biochemistry 31 (1992) 12304–12314.
[19] Z. Zhang, Y. Zhu, Y. Shi, Molecular dynamics simulations of urea and thermal-induced denaturation of S-peptide analogue, Biophys. Chem. 89 (2001) 145–162.
[20] N. Kumar, N. Kishore, Synergistic behavior of glycine betaine–urea mixture: a molecular dynamics study, J. Chem. Phys. 139 (2013) 115104.
[21] H.J.C. Berendsen, J.R. Grigera, T.P. Straatsma, The missing term in effective pair potentials, J. Phys. Chem. 91 (1987) 6269–6271.
[22] E.M. Duffy, P.J. Kowalczyk, W.L. Jorgensen, Do denaturants interact with aromatic hydrocarbons in water? J. Am. Chem. Soc. 115 (1993) 9271–9275.
[23] E.M. Duffy, D.L. Severance, W.L. Jorgensen, Urea: potential functions, log P, and free energy of hydration, Isr. J. Chem. 33 (1993) 323–330.
[24] D. Shukla, C. Shinde, B.L. Trout, Molecular computations of preferential interaction coefficients of proteins, J. Phys. Chem. B 113 (2009) 12546–12554.
[25] R. Sarma, S. Paul, Exploring the molecular mechanism of trimethylamine-N-oxide's ability to counteract the protein denaturing effects of urea, J. Phys. Chem. B 117 (2013) 5691–5704.
[26] H. Wei, Y. Fan, Y.Q. Gao, Effects of urea, tetramethyl urea, and trimethylamine N-oxide on aqueous solution structure and solvation of protein backbones: a molecular dynamics simulation study, J. Phys. Chem. B 114 (2010) 557–568.
[27] H.J.C. Berendsen, D. van der Spoel, R. van Drunen, GROMACS: a message-passing parallel molecular dynamics implementation, Comput. Phys. Commun. 91 (1995) 43–56.
[28] D. Van Der Spoel, E. Lindahl, B. Hess, G. Groenhof, A.E. Mark, H.J.C. Berendsen, GROMACS: fast, flexible, and free, J. Comput. Chem. 26 (2005) 1701–1718.
[29] B. Hess, C. Kutzner, D. van der Spoel, E. Lindahl, GROMACS 4: algorithms for highly efficient, load-balanced, and scalable molecular simulation, J. Chem. Theory Comput. 4 (2008) 435–447.
[30] H.J.C. Berendsen, J.P.M. Postma, W.F. van Gunsteren, A. DiNola, J.R. Haak, Molecular dynamics with coupling to an external bath, J. Chem. Phys. 81 (1984) 3684–3690.
[31] G. Bussi, D. Donadio, M. Parrinello, Canonical sampling through velocity rescaling, J. Chem. Phys. 126 (2007) 014101.
[32] B. Hess, H. Bekker, H.J.C. Berendsen, J.G.E.M. Fraaije, LINCS: a linear constraint solver for molecular simulations, J. Comput. Chem. 18 (1997) 1463–1472.
[33] U. Essmann, L. Perera, M.L. Berkowitz, T. Darden, H. Lee, L.G. Pedersen, A smooth particle mesh Ewald method, J. Chem. Phys. 103 (1995) 8577–8593.
[34] B.M. Baynes, B.L. Trout, Proteins in mixed solvents: a molecular-level perspective, J. Phys. Chem. B 107 (2003) 14058–14067.
[35] R. Gilman-Politi, D. Harries, Unraveling the molecular mechanism of enthalpy driven peptide folding by polyol osmolytes, J. Chem. Theory Comput. 7 (2011) 3816–3828.
[36] V. Vagenende, M.G.S. Yap, B.L. Trout, Molecular anatomy of preferential interaction coefficients by elucidating protein solvation in mixed solvents: methodology and application for lysozyme in aqueous glycerol, J. Phys. Chem. B 113 (2009) 11743–11753.
[37] W. Kabsch, C. Sander, Dictionary of protein secondary structure: pattern recognition of hydrogen-bonded and geometrical features, Biopolymers 22 (1983) 2577–2637.
[38] L.M. Samuelsson, J.J. Bedford, R.A.J. Smith, J.P. Leader, A comparison of the counteracting effects of glycine betaine and TMAO on the activity of RNase A in aqueous urea solution, Comp. Biochem. Physiol. A Comp. Physiol. 141 (2005) 22–28.
[39] D.W. Bolen, I.V. Baskakov, The osmophobic effect: natural selection of a thermodynamic force in protein folding, J. Mol. Biol. 310 (2001) 955–963.
[40] G. Saladino, M. Marenchino, S. Pieraccini, R. Campos-Olivas, M. Sironi, F.L. Gervasio, A simple mechanism underlying the effect of protecting osmolytes on protein folding, J. Chem. Theory Comput. 7 (2011) 3846–3852.
[41] L. Ma, L. Pegram, M.T. Record, Q. Cui, Preferential interactions between small solutes and the protein backbone: a computational analysis, Biochemistry 49 (2010) 1954–1962.
[42] M. Auton, D.W. Bolen, Predicting the energetics of osmolyte-induced protein folding/unfolding, Proc. Natl. Acad. Sci. 102 (2005) 15065–15068.
[43] G.A. Jeffrey, An Introduction to Hydrogen Bonding, Oxford University Press, New York, 1997.
[44] D. Tobi, R. Elber, D. Thirumalai, The dominant interaction between peptide and urea is electrostatic in nature: a molecular dynamics study, Biopolymers 68 (2003) 359–369.
[45] D. van der Spoel, P.J. van Maaren, P. Larsson, N. Timneanu, Thermodynamics of hydrogen bonding in hydrophilic and hydrophobic media, J. Phys. Chem. B 110 (2006) 4393–4398.
[46] M.C. Stumpe, H. Grubmüller, Aqueous urea solutions: structure, energetics, and urea aggregation, J. Phys. Chem. B 111 (2007) 6220–6228.
[47] Q. Zou, B.J. Bennion, V. Daggett, K.P. Murphy, The molecular mechanism of stabilization of proteins by TMAO and its ability to counteract the effects of urea, J. Am. Chem. Soc. 124 (2002) 1192–1202.
[48] E.J. Guinn, L.M. Pegram, M.W. Capp, M.N. Pollock, M.T. Record, Quantifying why urea is a protein denaturant, whereas glycine betaine is a protein stabilizer, Proc. Natl. Acad. Sci. 108 (2011) 16932–16937.
[49] C.Y. Hu, H. Kokubo, G.C. Lynch, D.W. Bolen, B.M. Pettitt, Backbone additivity in the transfer model of protein solvation, Protein Sci. 19 (2010) 1011–1022.
[50] M.C. Stumpe, H. Grubmuller, Interaction of urea with amino acids: implications for urea-induced protein denaturation, J. Am. Chem. Soc. 129 (2007) 16126–16131.
[51] L. Hua, R. Zhou, D. Thirumalai, B.J. Berne, Urea denaturation by stronger dispersion interactions with proteins than water implies a 2-stage unfolding, Proc. Natl. Acad. Sci. 105 (2008) 16928–16933.
[52] M. Auton, D.W. Bolen, J. Rösgen, Structural thermodynamics of protein preferential solvation: osmolyte solvation of proteins, aminoacids, and peptides, Proteins 73 (2008) 802–813.
[53] S. Paul, G.N. Patey, Hydrophobic interactions in urea-trimethylamine-N-oxide solutions, J. Phys. Chem. B 112 (2008) 11106–11111.
[54] N. Kumar, N. Kishore, Structure and effect of sarcosine on water and urea by using molecular dynamics simulations: Implications in protein stabilization, Biophys. Chem. 171 (2013) 9–15.